

# Measurements of CP violation in charmless 3-body B-meson decays at LHCb

Thomas Grammatico

Laboratoire de Physique Nucléaire et des Hautes Energies (LPNHE)

On behalf of the LHCb collaboration

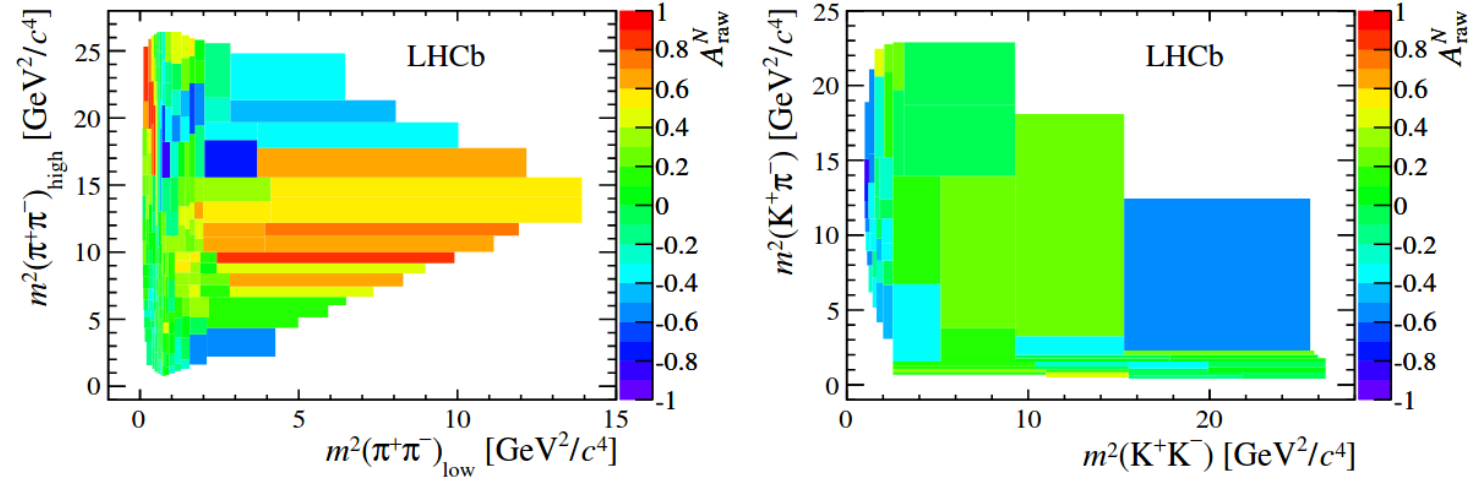
ICHEP

July 28 – August 6 2020



Large raw CP asymmetries were observed in both decays  
 [Phys. Rev. D 90, 112004 (2014)]

$$A_{\text{raw}}^N \equiv \frac{N^- - N^+}{N^- + N^+}$$



→ This result provides a strong motivation to perform amplitude analyses:

- $B^\pm \rightarrow \pi^\pm K^+ K^-$  [Phys. Rev. Letters 123,231802 (2019)]
- $B^+ \rightarrow \pi^+ \pi^+ \pi^-$  [Phys. Rev. D 101,012006 (2020)]  
 [Phys. Rev. Lett. 124 (2020) 031801]

3 fb<sup>-1</sup> data sample (2011 and 2012)

The decays are coupled through rescattering process  $\pi\pi \leftrightarrow KK$

Rescattering: a pair of meson produced in one channel will appear in the coupled decay

# Amplitude analyses of $B^\pm \rightarrow \pi^\pm K^+ K^-$ and $B^+ \rightarrow \pi^+ \pi^+ \pi^-$ decays

$B^+ \rightarrow \pi^+ \pi^+ \pi^-$  S-wave amplitude described by three approaches:

- Isobar model:

$$A^+ = \sum_j^N c_j^+ F_j(m_{13}^2, m_{23}^2)$$

CP conserving

$$A^- = \sum_j^N c_j^- F_j(m_{13}^2, m_{23}^2)$$

CP violating

Breit-Wiegner x Angular dependence x barrier factors

$$F(m_{13}^2, m_{23}^2) \propto R(m_{13}) \cdot T(\vec{p}, \vec{q}) \cdot X(|\vec{p}|r_{BW}^P) \cdot X(|\vec{q}|r_{BW}^R)$$

$$c_j^\pm = (x \pm \delta x) + i(y \pm \delta y)$$

CP violating

- K-matrix formalism: [Ann. Phys. (N.Y.)507, 404 (1995)], [Ann. Phys. (N.Y.)10, 307 (1960)], [Nucl. Phys.A189, 417 (1972)]

When the dynamics is dominated by 2-body processes → 2-body unitarity is conserved in this formalism  
 The produced initial states are propagated to the observed final state by the K-matrix term

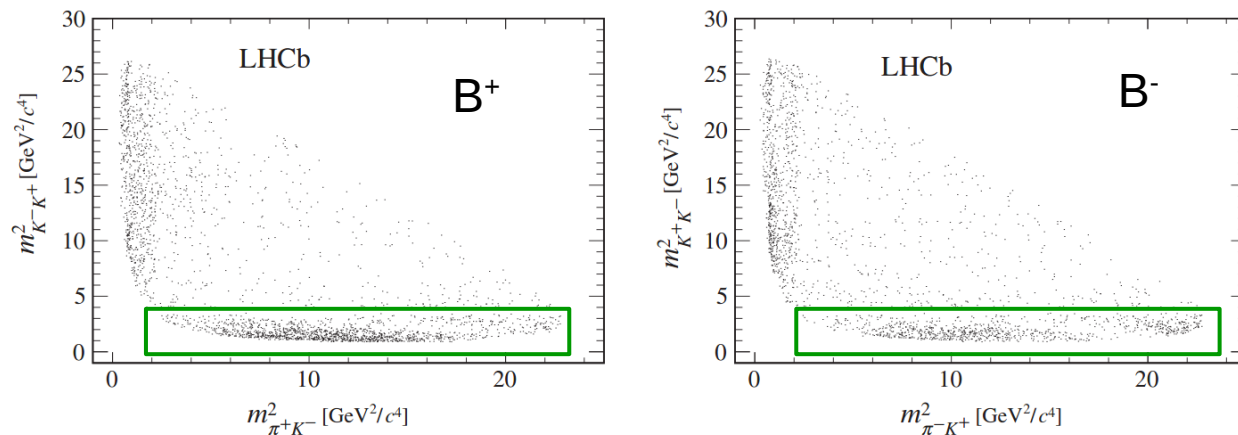
- Quasi-model-independent procedure: [Phys. Rev.D74, 059901 (2006)], [Phys. Rev. D78,052001 (2008)], [Phys. Lett. B681,14 (2009)], [Phys.Rev. D83, 072001 (2011)], [Phys. Rev. D79, 032003(2009)], [Phys. Rev. D94, 072001 (2016)]

The S-wave is described by binned amplitudes and phases  
 The S-wave amplitude is constant in  $\cos(\theta_{hel})$  → allows to separate the S-wave from the other contributions

Isobar model used to describe the other amplitudes

# Amplitude analysis of $B^\pm \rightarrow \pi^\pm K^+ K^-$ decays

[Phys. Rev. Letters 123,231802 (2019)]



Signal yield  
 $2052 \pm 102$  ( $1566 \pm 84$ )  $B^+$  ( $B^-$ )

First amplitude analysis of this mode

CPV effects clearly visible when comparing  $B^+$  and  $B^-$  distributions

Resonant contributions are limited:

- $\pi K$  resonances from penguin diagram only
- $KK$  resonances from both tree level and penguin diagram can occur.  
The  $s\bar{s}$  contribution is suppressed by OZI rule

$B^+$  and  $B^-$  are fitted simultaneously allowing for CPV

# Amplitude analysis of $B^\pm \rightarrow \pi^\pm K^+ K^-$ decays – Results [Phys. Rev. Letters 123,231802 (2019)]

3 contributions in the  $\pi K$  system

4 contributions in the  $KK$  system

Contribution	Fit fraction (%)	$A_{CP}$ (%)	Magnitude ( $B^+/B^-$ )	Phase [ $^\circ$ ] ( $B^+/B^-$ )
$K^*(892)^0$	$7.5 \pm 0.6 \pm 0.5$	$+12.3 \pm 8.7 \pm 4.5$	$0.94 \pm 0.04 \pm 0.02$ $1.06 \pm 0.04 \pm 0.02$	0 (fixed) 0 (fixed)
$K_0^*(1430)^0$	$4.5 \pm 0.7 \pm 1.2$	$+10.4 \pm 14.9 \pm 8.8$	$0.74 \pm 0.09 \pm 0.09$ $0.82 \pm 0.09 \pm 0.10$	$-176 \pm 10 \pm 16$ $136 \pm 11 \pm 21$
Single pole	<b><math>32.3 \pm 1.5 \pm 4.1</math></b>	$-10.7 \pm 5.3 \pm 3.5$	$2.19 \pm 0.13 \pm 0.17$ $1.97 \pm 0.12 \pm 0.20$	$-138 \pm 7 \pm 5$ $166 \pm 6 \pm 5$
$\rho(1450)^0$	$30.7 \pm 1.2 \pm 0.9$	$-10.9 \pm 4.4 \pm 2.4$	$2.14 \pm 0.11 \pm 0.07$ $1.92 \pm 0.10 \pm 0.07$	$-175 \pm 10 \pm 15$ $140 \pm 13 \pm 20$
$f_2(1270)$	$7.5 \pm 0.8 \pm 0.7$	$+26.7 \pm 10.2 \pm 4.8$	$0.86 \pm 0.09 \pm 0.07$ $1.13 \pm 0.08 \pm 0.05$	$-106 \pm 11 \pm 10$ $-128 \pm 11 \pm 14$
Rescattering	$16.4 \pm 0.8 \pm 1.0$	<b><math>-66.4 \pm 3.8 \pm 1.9</math></b>	$1.91 \pm 0.09 \pm 0.06$ $0.86 \pm 0.07 \pm 0.04$	$-56 \pm 12 \pm 18$ $-81 \pm 14 \pm 15$
$\phi(1020)$	$0.3 \pm 0.1 \pm 0.1$	$+9.8 \pm 43.6 \pm 26.6$	$0.20 \pm 0.07 \pm 0.02$ $0.22 \pm 0.06 \pm 0.04$	$-52 \pm 23 \pm 32$ $107 \pm 33 \pm 41$

$$A_{CP_i} = \frac{|\bar{c}_i|^2 - |c_i|^2}{|\bar{c}_i|^2 + |c_i|^2}$$

$$FF_i = \frac{\int (|c_i F_i|^2 + |\bar{c}_i \bar{F}_i|^2) dm_{\pi^\pm K^\mp}^2 dm_{K^+ K^-}^2}{\int (|A|^2 + |\bar{A}|^2) dm_{\pi^\pm K^\mp}^2 dm_{K^+ K^-}^2}$$

Non resonant amplitude → phenomenological description of the partonic interaction

Single-pole form factor described as:

$$[1 + m^2(\pi^\pm K^\mp)/\Lambda^2]^{-1}$$

[Phys. Rev. D 92, 054010] Largest fit fraction

Rescattering: single-pole x scattering term  $\sqrt{1 - v^2} e^{2i\delta}$

[Phys. Rev. D 71, 074016]

Large CP asymmetry in the  $\pi\pi \leftrightarrow KK$  rescattering contribution

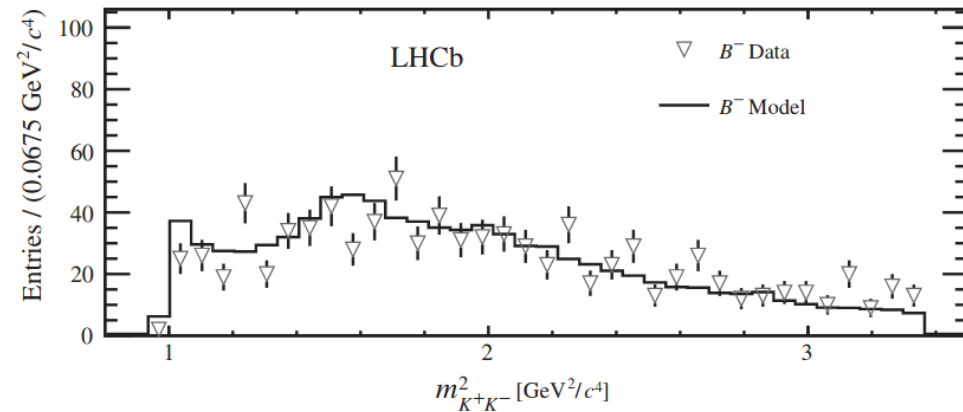
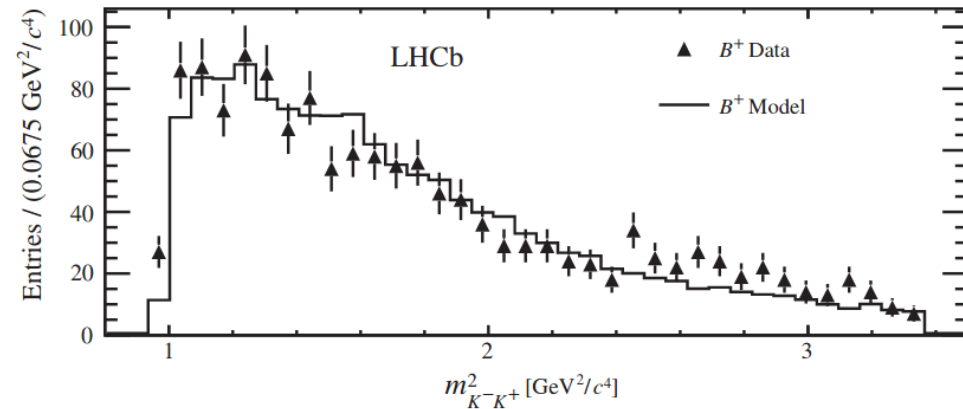
# Amplitude analysis of $B^\pm \rightarrow \pi^\pm K^+ K^-$ decays – Results [Phys. Rev. Letters 123,231802 (2019)]

S-wave rescattering amplitude gives a **CPV** of  **$(-66 \pm 4 \pm 2)\%$**

**Largest CPV** observation for a **single amplitude**

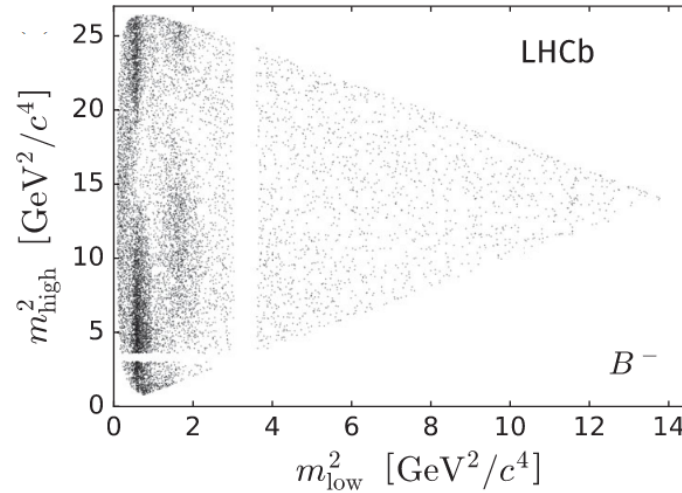
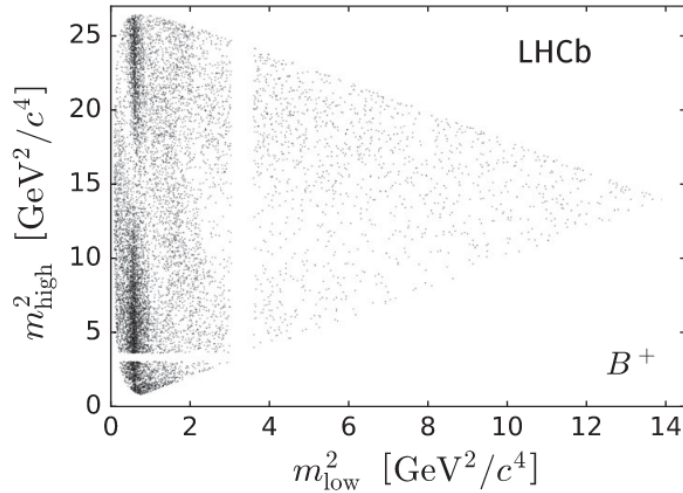
The **CPV** observed in the **rescattering** process is **consistent** with the positive CPV in the coupled mode  $B^+ \rightarrow \pi^+ \pi^+ \pi^-$

$B \rightarrow \rho(1450)^0 \pi$  **fit fraction** is  **$\sim 30\%$**   
→ larger than expected, Run 2 data will help to further scrutinise this effect



# Amplitude analysis of $B^+ \rightarrow \pi^+ \pi^+ \pi^-$ decays

[Phys. Rev. D 101,012006 (2020)]  
[Phys. Rev. Lett. 124 (2020) 031801]



Signal yield  $20600 \pm 1600$

$B^+ \rightarrow \pi_1^+ \pi_2^+ \pi_3^-$  decay amplitude is expressed as a function of  $m_{13}^2$  and  $m_{23}^2$

Bose symmetry  $\rightarrow A(m_{13}^2, m_{23}^2) \equiv A(m_{23}^2, m_{13}^2) \rightarrow \pi_1$  and  $\pi_2$  can be assigned arbitrarily

$\rightarrow$  Natural foldings along  $m_{13}^2 = m_{23}^2$

# Amplitude analysis of $B^+ \rightarrow \pi^+ \pi^+ \pi^-$ decays – Results

[Phys. Rev. D 101,012006 (2020)]  
[Phys. Rev. Lett. 124 (2020) 031801]

## CP-averaged fit fractions $\mathcal{F}_j$

Component	Isobar	K-matrix	QMI
$\rho(770)^0$	$55.5 \pm 0.6 \pm 0.4 \pm 2.5$	$56.5 \pm 0.7 \pm 1.5 \pm 3.1$	$54.8 \pm 1.0 \pm 1.9 \pm 1.0$
$\omega(782)$	$0.50 \pm 0.03 \pm 0.01 \pm 0.04$	$0.47 \pm 0.04 \pm 0.01 \pm 0.03$	$0.57 \pm 0.10 \pm 0.12 \pm 0.12$
$f_2(1270)$	$9.0 \pm 0.3 \pm 0.7 \pm 1.4$	$9.3 \pm 0.4 \pm 0.6 \pm 2.4$	$9.6 \pm 0.4 \pm 0.7 \pm 3.9$
$\rho(1450)^0$	$5.2 \pm 0.3 \pm 0.2 \pm 1.9$	$10.5 \pm 0.7 \pm 0.8 \pm 4.5$	$7.4 \pm 0.5 \pm 3.9 \pm 1.1$
$\rho_3(1690)^0$	$0.5 \pm 0.1 \pm 0.1 \pm 0.3$	$1.5 \pm 0.1 \pm 0.1 \pm 0.4$	$1.0 \pm 0.1 \pm 0.5 \pm 0.1$
S-wave	$25.4 \pm 0.5 \pm 0.5 \pm 3.6$	$25.7 \pm 0.6 \pm 2.6 \pm 1.4$	$26.8 \pm 0.7 \pm 2.0 \pm 1.0$

Dominant contributions

## Quasi 2-body CP asymmetries $\mathcal{A}_{CP}^j$

Component	Isobar	K-matrix	QMI
$\rho(770)^0$	$+0.7 \pm 1.1 \pm 0.6 \pm 1.5$	$+4.2 \pm 1.5 \pm 2.6 \pm 5.8$	$+4.4 \pm 1.7 \pm 2.3 \pm 1.6$
$\omega(782)$	$-4.8 \pm 6.5 \pm 1.3 \pm 3.5$	$-6.2 \pm 8.4 \pm 5.6 \pm 8.1$	$-7.9 \pm 16.5 \pm 14.2 \pm 7.0$
$f_2(1270)$	$+46.8 \pm 6.1 \pm 1.5 \pm 4.4$	$+42.8 \pm 4.1 \pm 2.1 \pm 8.9$	$+37.6 \pm 4.4 \pm 6.0 \pm 5.2$
$\rho(1450)^0$	$-12.9 \pm 3.3 \pm 3.6 \pm 35.7$	$+9.0 \pm 6.0 \pm 10.8 \pm 45.7$	$-15.5 \pm 7.3 \pm 14.3 \pm 32.2$
$\rho_3(1690)^0$	$-80.1 \pm 11.4 \pm 7.8 \pm 24.1$	$-35.7 \pm 10.8 \pm 8.5 \pm 35.9$	$-93.2 \pm 6.8 \pm 8.0 \pm 38.1$
S-wave	$+14.4 \pm 1.8 \pm 1.0 \pm 1.9$	$+15.8 \pm 2.6 \pm 2.1 \pm 6.9$	$+15.0 \pm 2.7 \pm 4.2 \pm 7.0$

No CPV observed

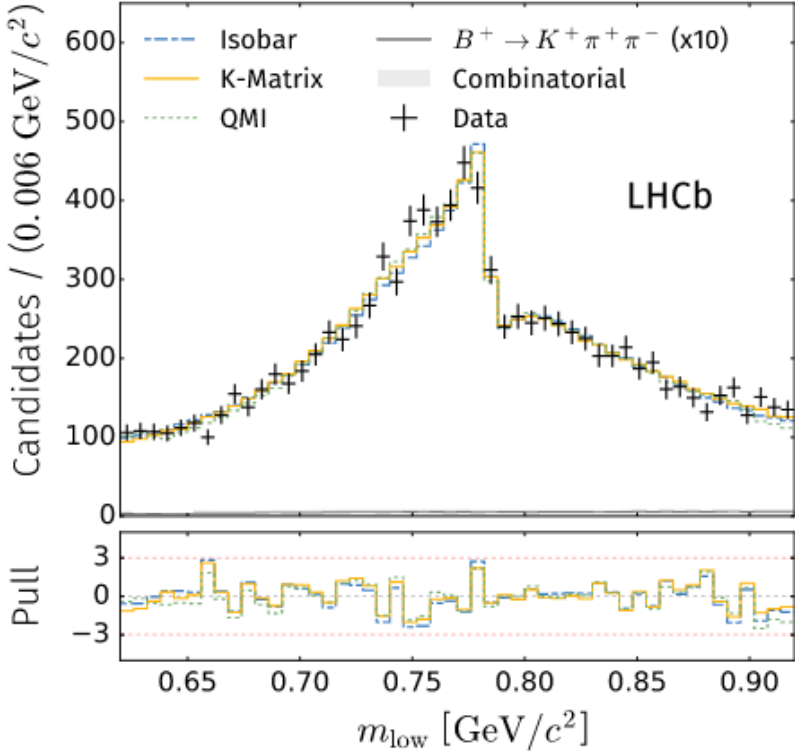
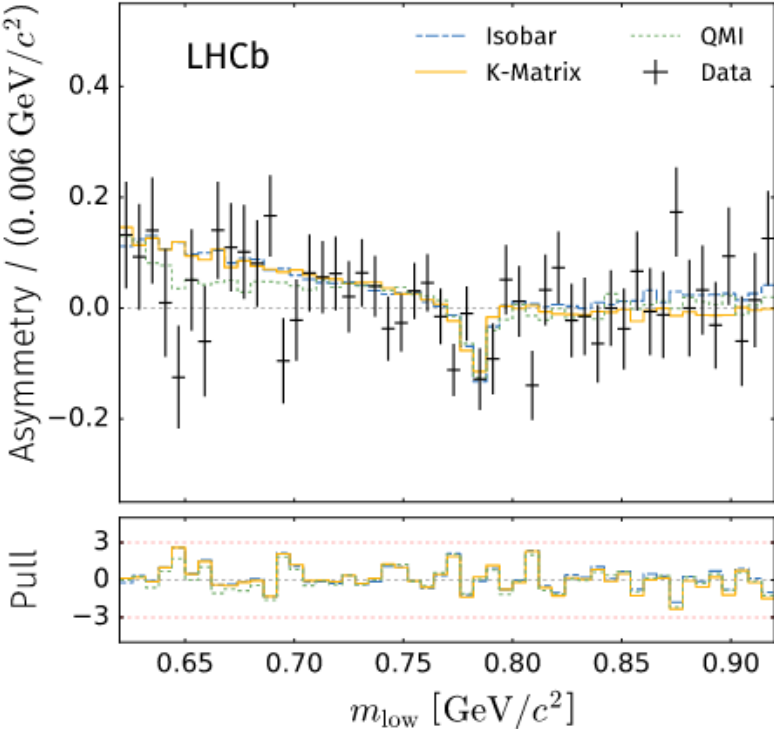
First CPV observation in a process involving a tensor

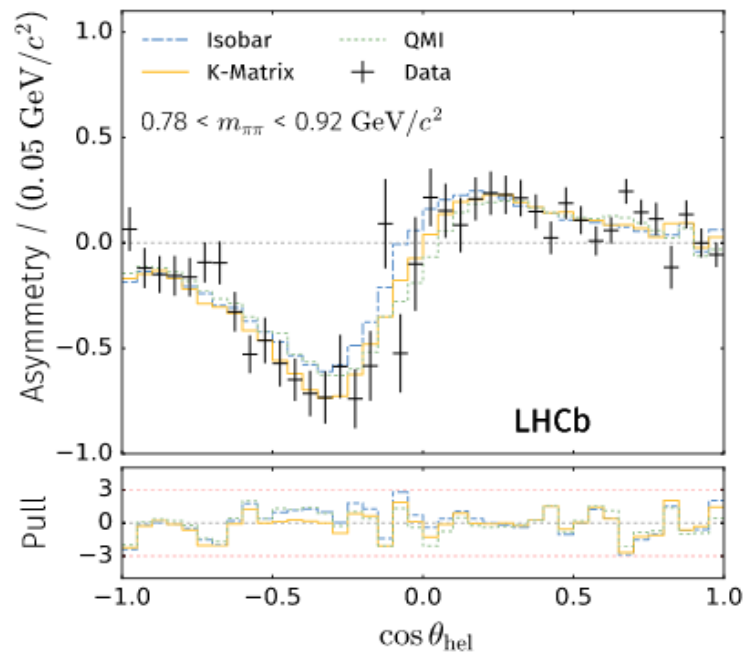
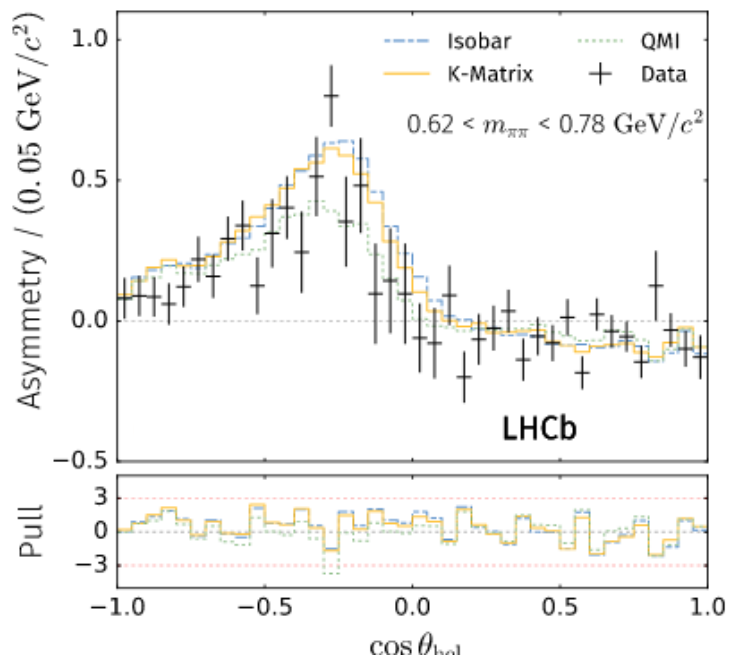
$$\mathcal{A}_{CP}^j = \frac{|c_j^-|^2 - |c_j^+|^2}{|c_j^-|^2 + |c_j^+|^2}$$

$$\mathcal{F}_j = \frac{\int_{\text{DP}} (|A_j^+(m_{13}^2, m_{23}^2)|^2 + |A_j^-(m_{13}^2, m_{23}^2)|^2) dm_{13}^2 dm_{23}^2}{\int_{\text{DP}} (|A^+(m_{13}^2, m_{23}^2)|^2 + |A^-(m_{13}^2, m_{23}^2)|^2) dm_{13}^2 dm_{23}^2}$$

The 3 approaches (isobar model, K-matrix formalism and QMI procedure) are in good agreement

No significant CPV observed in the  $\rho(770)$ - $\omega(782)$  region when integrating over  $\cos(\theta_{hel})$

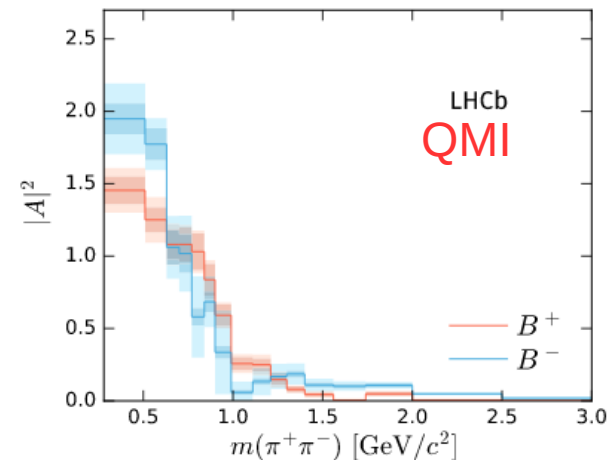
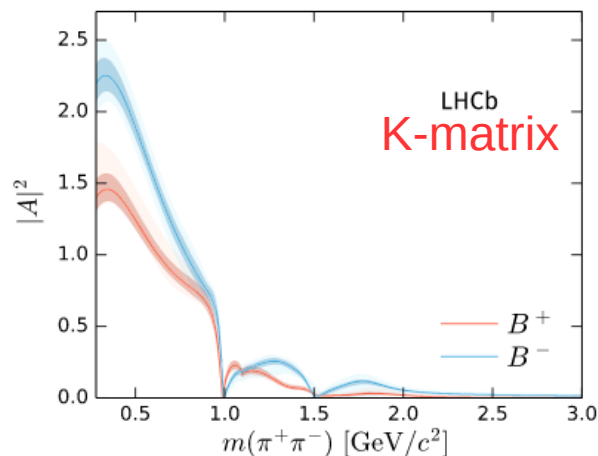
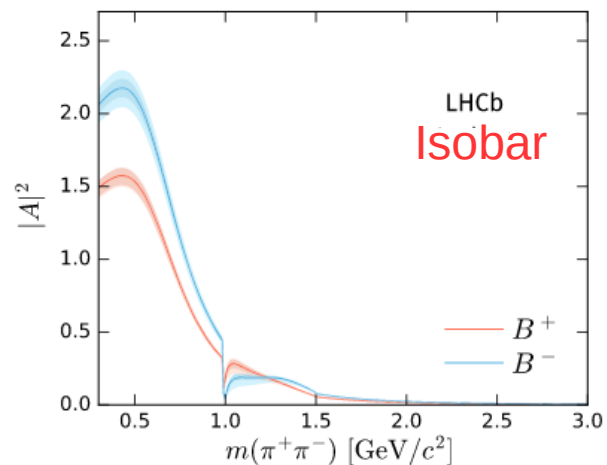




Significant CPV observed in the  $\cos(\theta_{\text{hel}})$  projection that changes sign on each side of the  $\rho$  peak  
 Expected when the spin-1  $\rho$  resonance interferes with a broad spin 0 component  
 Cancels when integrating over the helicity angle and/or invariant mass

# Amplitude analysis of $B^+ \rightarrow \pi^+\pi^+\pi^-$ decays - The $\pi\pi$ S-wave

[Phys. Rev. D 101,012006 (2020)]  
[Phys. Rev. Lett. 124 (2020) 031801]



The 3 approaches (IsoBar model, K-matrix, QMI) are consistent with each other

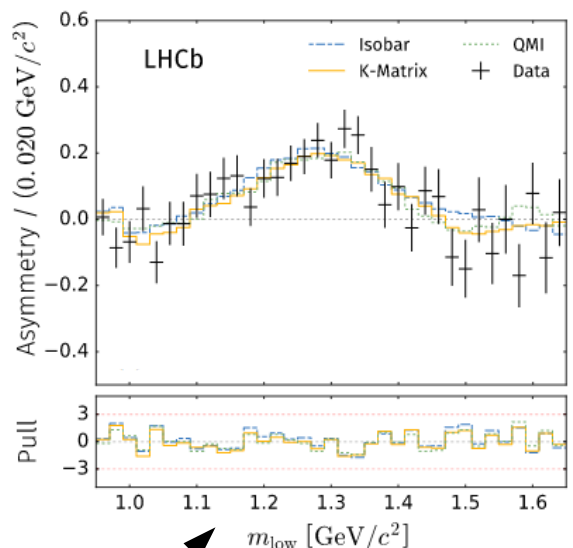
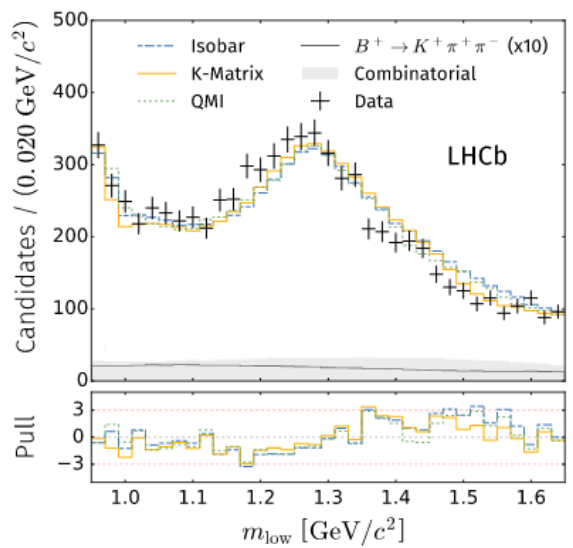
Clear CP asymmetry below  $K^+K^-$  threshold, where it changes sign

# Amplitude analysis of $B^+ \rightarrow \pi^+\pi^+\pi^-$ decays - The $f_2(1270)$ region

[Phys. Rev. D 101,012006 (2020)]  
 [Phys. Rev. Lett. 124 (2020) 031801]

Acp

Component	Isobar	K-matrix	QMI
$f_2(1270)$	$+46.8 \pm 6.1 \pm 1.5 \pm 4.4$	$+42.8 \pm 4.1 \pm 2.1 \pm 8.9$	$+37.6 \pm 4.4 \pm 6.0 \pm 5.2$



First CP asymmetry observed in a process involving a tensor

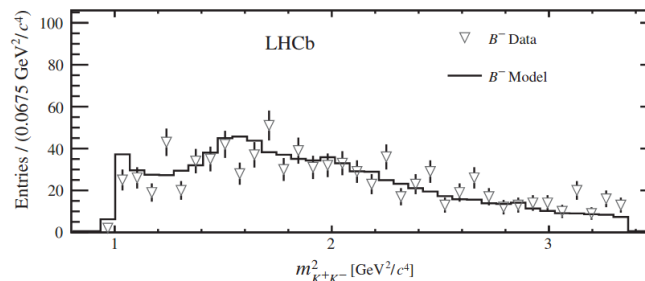
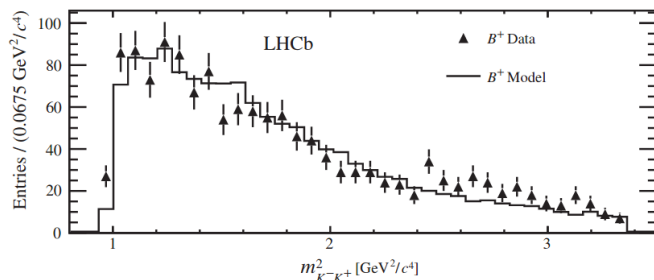
Robust result with respect to the experimental and model uncertainties

# Summary

Challenging amplitude analyses were performed to better understand the CP violation observed in  $B^\pm \rightarrow \pi^\pm K^+ K^-$  and  $B^+ \rightarrow \pi^+ \pi^+ \pi^-$  decays

$B^\pm \rightarrow \pi^\pm K^+ K^-$  [Phys. Rev. Letters 123,231802 (2019)]

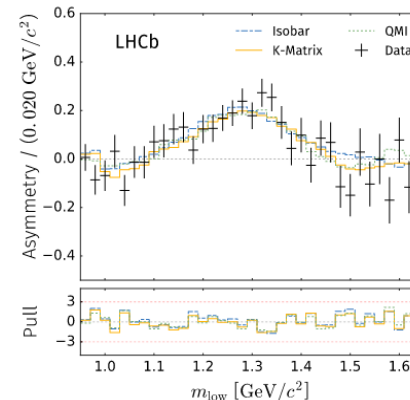
**Large CP violation** observed in the S-wave contribution – consistent with what is observed in  $B^+ \rightarrow \pi^+ \pi^+ \pi^-$



$B^+ \rightarrow \pi^+ \pi^+ \pi^-$  [Phys. Rev. D 101,012006 (2020)], [Phys. Rev. Lett. 124 (2020) 031801]  
S-wave contribution described by 3 consistent approaches

**CP violation** observed in the **S-wave** and in the **interferences** between the **S- and the P-wave**

**First CP violation** observed in a process involving a **tensor**

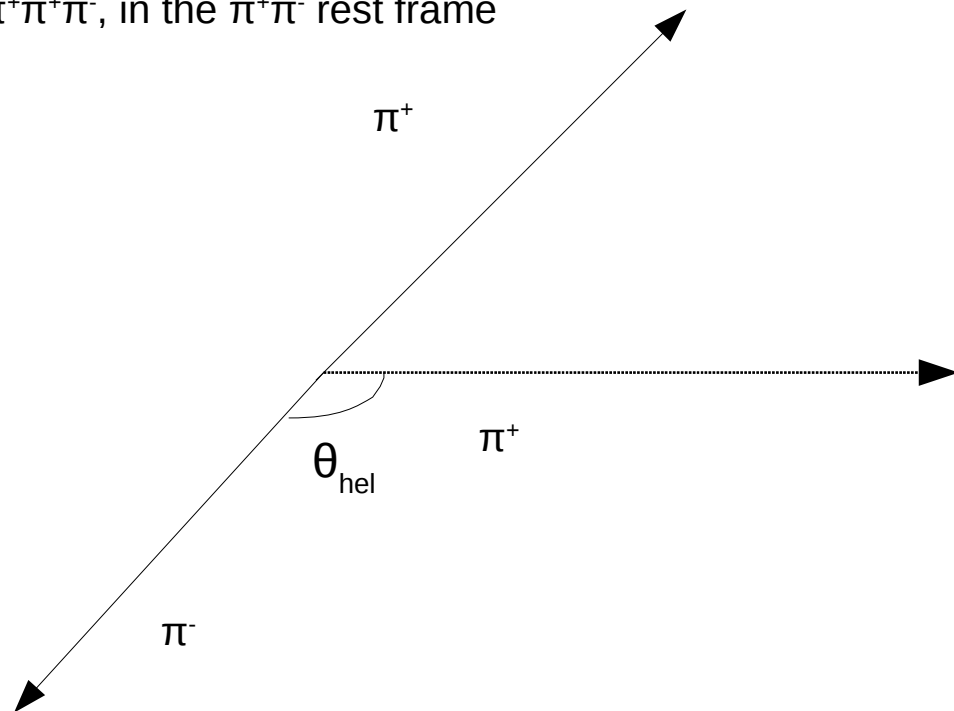


**Run 2 should bring new exciting insights on these decays**

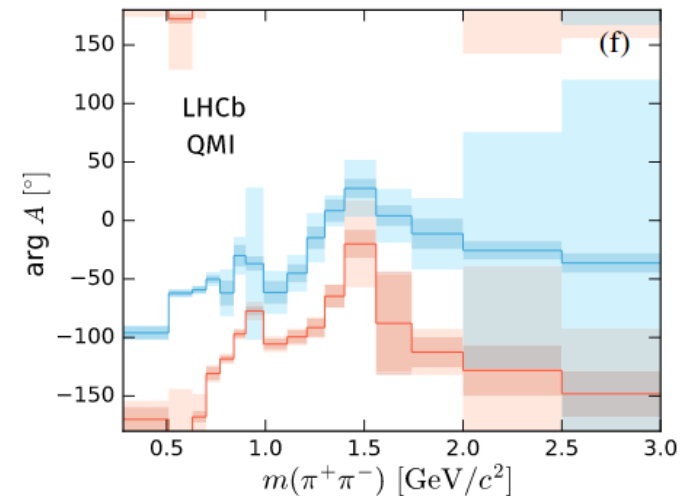
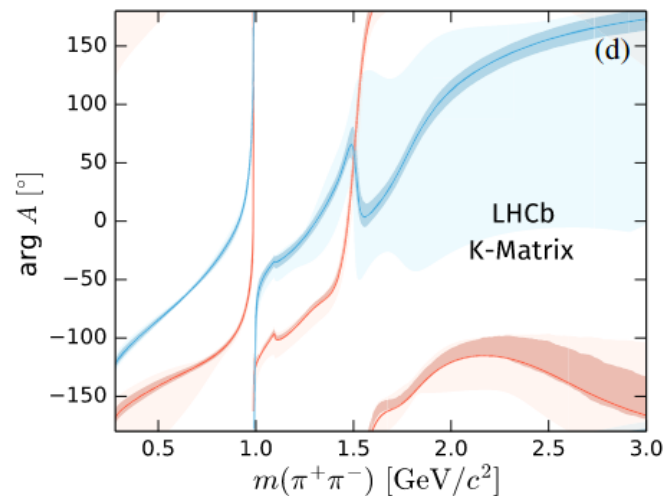
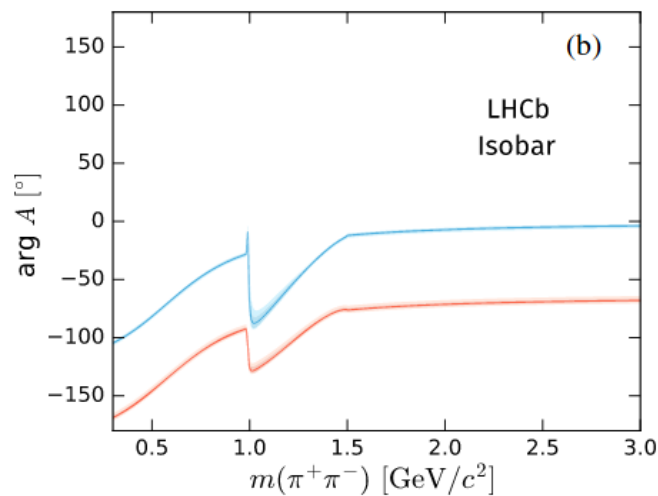
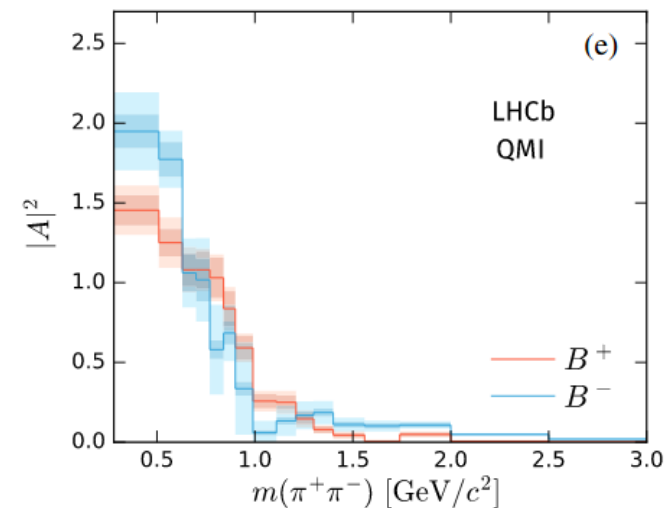
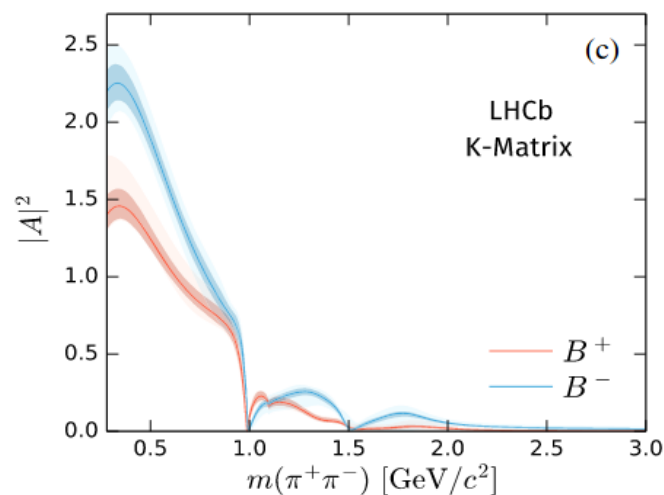
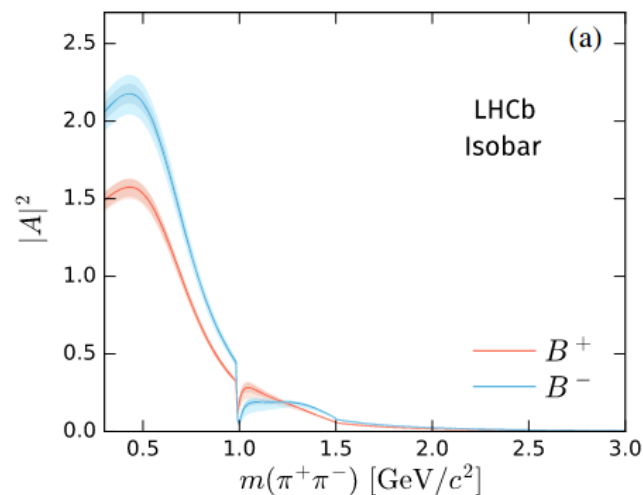
# Backup

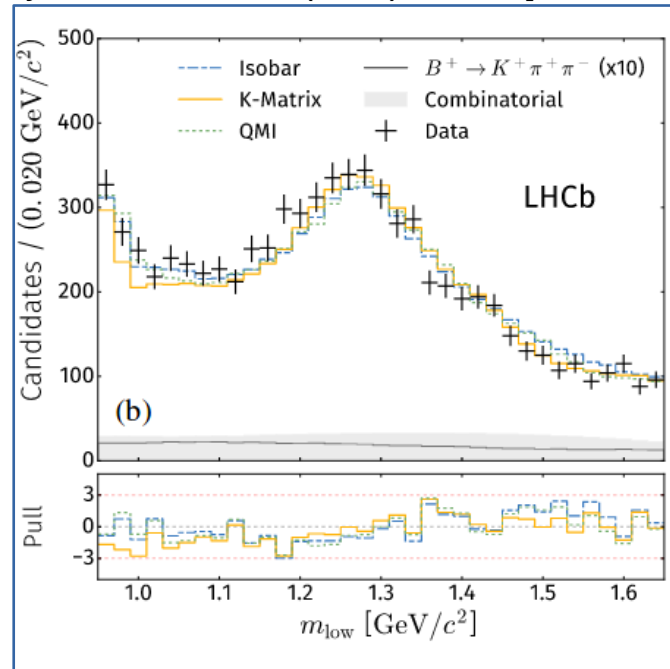
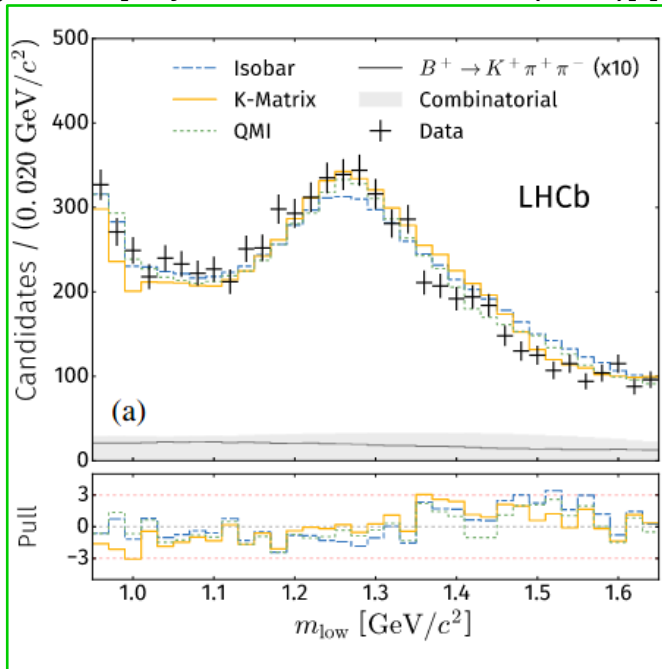
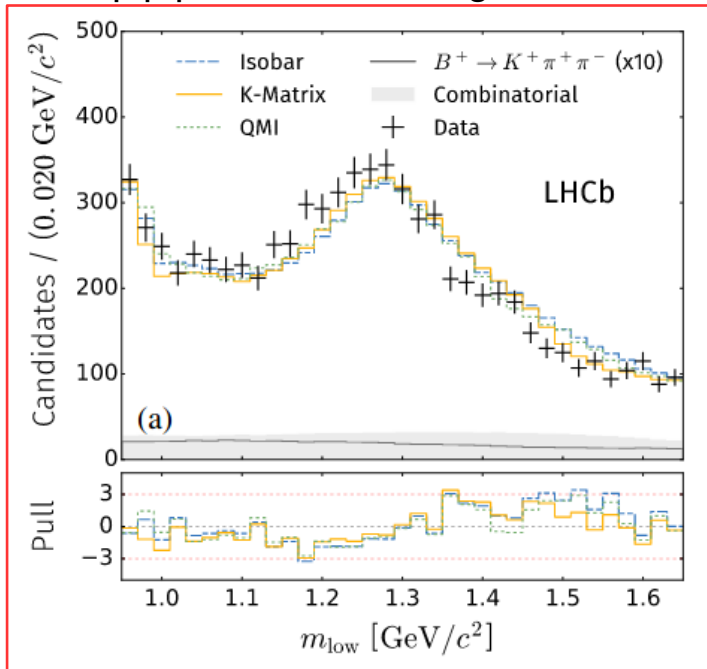
Theta Helicity angle

For  $B^+ \rightarrow \pi^+\pi^+\pi^-$ , in the  $\pi^+\pi^-$  rest frame



The  $\pi\pi$  S-wave – phase motion [Phys. Rev. D 101,012006 (2020)], [Phys. Rev. Lett. 124 (2020) 031801]





Clear discrepancy with the data in the  $f_2(1270)$  region

Better agreement when mass and width of the  $f_2$  are allowed to vary but mass  $4\sigma$  away from world average

Addition of a second spin-2 state  $f_2(1430)$  reduces the discrepancy - not added to the baseline but used to evaluate systematics

J. Backet et al., Laura++: A Dalitz plot fitter, [Comput. Phys.Commun.231, 198 (2018)]

B. Aubert et al. (BABAR Collaboration) Dalitz plot analysis of  $B^\pm \rightarrow \pi^\pm \pi^\pm \pi^\mp$  decays [Phys. Rev. D72,052002 (2005)],[Phys. Rev. D79,072006 (2009)]

[Phys. Rev. D72,052002 (2005)],[Phys. Rev. D79,072006 (2009)]

Mode	Fit Fraction (%)	$\mathcal{B}(B^\pm \rightarrow \text{Mode})(10^{-6})$	$\mathcal{A}_{CP}$ (%)
$\pi^\pm \pi^\pm \pi^\mp$ Total		$15.2 \pm 0.6 \pm 1.2^{+0.4}_{-0.3}$	$+3.2 \pm 4.4 \pm 3.1^{+2.5}_{-2.0}$
$\rho^0(770)\pi^\pm; \rho^0(770) \rightarrow \pi^+\pi^-$	$53.2 \pm 3.7 \pm 2.5^{+1.5}_{-7.4}$	$8.1 \pm 0.7 \pm 1.2^{+0.4}_{-1.1}$	$+18 \pm 7 \pm 5^{+2}_{-14}$
$\rho^0(1450)\pi^\pm; \rho^0(1450) \rightarrow \pi^+\pi^-$	$9.1 \pm 2.3 \pm 2.4^{+1.9}_{-4.5}$	$1.4 \pm 0.4 \pm 0.4^{+0.3}_{-0.7}$	$-6 \pm 28 \pm 20^{+12}_{-35}$
$f_2(1270)\pi^\pm; f_2(1270) \rightarrow \pi^+\pi^-$	$5.9 \pm 1.6 \pm 0.4^{+2.0}_{-0.7}$	$0.9 \pm 0.2 \pm 0.1^{+0.3}_{-0.1}$	$+41 \pm 25 \pm 13^{+12}_{-8}$
$f_0(1370)\pi^\pm; f_0(1370) \rightarrow \pi^+\pi^-$	$18.9 \pm 3.3 \pm 2.6^{+4.3}_{-3.5}$	$2.9 \pm 0.5 \pm 0.5^{+0.7}_{-0.5} (< 4.0)$	$+72 \pm 15 \pm 14^{+7}_{-8}$
$\pi^\pm \pi^\pm \pi^\mp$ nonresonant	$34.9 \pm 4.2 \pm 2.9^{+7.5}_{-3.4}$	$5.3 \pm 0.7 \pm 0.6^{+1.1}_{-0.5}$	$-14 \pm 14 \pm 7^{+17}_{-3}$
$f_0(980)\pi^\pm; f_0(980) \rightarrow \pi^+\pi^-$	-	$< 1.5$	-
$\chi_{c0}\pi^\pm; \chi_{c0} \rightarrow \pi^+\pi^-$	-	$< 0.1$	-
$\chi_{c2}\pi^\pm; \chi_{c2} \rightarrow \pi^+\pi^-$	-	$< 0.1$	-

Component	Isobar	$K$ -matrix	QMI
$\rho(770)^0$	$55.5 \pm 0.6 \pm 0.4 \pm 2.5$	$56.5 \pm 0.7 \pm 1.5 \pm 3.1$	$54.8 \pm 1.0 \pm 1.9 \pm 1.0$
$\omega(782)$	$0.50 \pm 0.03 \pm 0.01 \pm 0.04$	$0.47 \pm 0.04 \pm 0.01 \pm 0.03$	$0.57 \pm 0.10 \pm 0.12 \pm 0.12$
$f_2(1270)$	$9.0 \pm 0.3 \pm 0.7 \pm 1.4$	$9.3 \pm 0.4 \pm 0.6 \pm 2.4$	$9.6 \pm 0.4 \pm 0.7 \pm 3.9$
$\rho(1450)^0$	$5.2 \pm 0.3 \pm 0.2 \pm 1.9$	$10.5 \pm 0.7 \pm 0.8 \pm 4.5$	$7.4 \pm 0.5 \pm 3.9 \pm 1.1$
$\rho_3(1690)^0$	$0.5 \pm 0.1 \pm 0.1 \pm 0.3$	$1.5 \pm 0.1 \pm 0.1 \pm 0.4$	$1.0 \pm 0.1 \pm 0.5 \pm 0.1$
$S$ -wave	$25.4 \pm 0.5 \pm 0.5 \pm 3.6$	$25.7 \pm 0.6 \pm 2.6 \pm 1.4$	$26.8 \pm 0.7 \pm 2.0 \pm 1.0$

Component	Isobar	$K$ -matrix	QMI
$\rho(770)^0$	$+0.7 \pm 1.1 \pm 0.6 \pm 1.5$	$+4.2 \pm 1.5 \pm 2.6 \pm 5.8$	$+4.4 \pm 1.7 \pm 2.3 \pm 1.6$
$\omega(782)$	$-4.8 \pm 6.5 \pm 1.3 \pm 3.5$	$-6.2 \pm 8.4 \pm 5.6 \pm 8.1$	$-7.9 \pm 16.5 \pm 14.2 \pm 7.0$
$f_2(1270)$	$+46.8 \pm 6.1 \pm 1.5 \pm 4.4$	$+42.8 \pm 4.1 \pm 2.1 \pm 8.9$	$+37.6 \pm 4.4 \pm 6.0 \pm 5.2$
$\rho(1450)^0$	$-12.9 \pm 3.3 \pm 3.6 \pm 35.7$	$+9.0 \pm 6.0 \pm 10.8 \pm 45.7$	$-15.5 \pm 7.3 \pm 14.3 \pm 32.2$
$\rho_3(1690)^0$	$-80.1 \pm 11.4 \pm 7.8 \pm 24.1$	$-35.7 \pm 10.8 \pm 8.5 \pm 35.9$	$-93.2 \pm 6.8 \pm 8.0 \pm 38.1$
$S$ -wave	$+14.4 \pm 1.8 \pm 1.0 \pm 1.9$	$+15.8 \pm 2.6 \pm 2.1 \pm 6.9$	$+15.0 \pm 2.7 \pm 4.2 \pm 7.0$

[Phys. Rev. D 101,012006 (2020)],[Phys. Rev. Lett. 124 (2020) 031801]

TABLE IV. Systematic uncertainties on the  $CP$ -averaged fit fractions, given in units of  $10^{-2}$ , for the isobar method. Uncertainties are given both for the total  $S$ -wave, and for the individual components due to the  $\sigma$  pole and the rescattering amplitude. For comparison, the statistical uncertainties are also listed at the bottom.

Category	$\rho(770)^0$	$\omega(782)$	$f_2(1270)$	$\rho(1450)^0$	$\rho_3(1690)^0$	$S$ -wave	Rescattering	$\sigma$
$B$ mass fit	0.23	0.01	0.68	0.07	0.03	0.40	0.16	0.02
Efficiency								
Simulation sample size	0.10	<0.01	0.06	0.05	0.01	0.08	0.02	0.09
Binning	0.07	<0.01	0.03	0.08	0.02	0.09	0.01	0.08
L0 Trigger	0.02	<0.01	<0.01	<0.01	<0.01	0.02	<0.01	0.02
Combinatorial bkgd	0.26	<0.01	0.14	0.15	0.03	0.28	0.04	0.31
$B^+ \rightarrow K^+ \pi^+ \pi^-$	0.01	<0.01	<0.01	<0.01	<0.01	0.01	<0.01	0.01
Fit bias	0.03	<0.01	0.01	0.01	0.01	0.04	<0.01	0.04
Total experimental	0.4	0.0	0.7	0.2	0.1	0.5	0.2	0.3
Amplitude model								
Resonance properties	0.63	0.01	0.17	0.39	0.05	0.29	0.01	0.41
Barrier factors	0.82	0.01	0.18	0.40	0.01	0.05	0.04	0.17
Alternative line shapes								
$f_2(1270)$	0.23	<0.01	0.68	0.07	0.03	0.40	0.16	0.02
$f_2(1430)$	0.40	<0.01	0.88	0.25	0.10	0.90	0.21	0.66
$\rho(1700)^0$	0.88	0.02	0.09	1.28	0.01	0.01	<0.01	<0.01
Isobar specifics								
$\sigma$ from PDG	2.00	0.03	0.69	1.18	0.32	3.40	0.35	4.90
Rescattering	0.01	<0.01	0.19	0.03	<0.01	0.11	0.07	0.24
Total model	2.5	0.0	1.4	1.9	0.3	3.6	0.5	5.0
Statistical uncertainty	0.6	0.0	0.3	0.3	0.1	0.5	0.2	0.5

[Phys. Rev. D 101,012006  
(2020)], [Phys. Rev. Lett. 124  
(2020) 031801]

TABLE V. Systematic uncertainties on  $\mathcal{A}_{CP}$  values, given in units of  $10^{-2}$ , for the isobar method. Uncertainties are given both for the total  $S$ -wave, and for the individual components due to the  $\sigma$  pole and the rescattering amplitude. For comparison, the statistical uncertainties are also listed at the bottom.

Category	$\rho(770)^0$	$\omega(782)$	$f_2(1270)$	$\rho(1450)^0$	$\rho_3(1690)^0$	$S$ -wave	Rescattering	$\sigma$
$B$ mass fit	0.12	0.10	0.89	0.40	4.19	0.58	4.20	0.54
Efficiency								
Simulation sample size	0.34	0.71	0.61	0.92	1.24	0.36	1.00	0.35
Binning	0.27	0.87	0.23	1.19	0.52	0.28	1.43	0.22
L0 Trigger	0.02	0.37	0.17	0.31	0.28	0.14	0.32	0.19
Combinatorial bkgd	0.40	0.50	1.02	3.06	5.75	0.75	3.16	0.75
$B^+ \rightarrow K^+ \pi^+ \pi^-$	<0.01	0.01	0.02	0.03	0.05	0.01	0.04	0.01
Fit bias	0.05	0.35	0.25	1.10	2.95	0.04	0.96	0.09
Total experimental	0.6	1.3	1.5	3.6	7.8	1.0	5.5	1.0
Amplitude model								
Resonance properties	0.20	0.53	0.55	2.66	5.58	0.41	1.58	0.29
Barrier factors	0.18	0.95	0.80	3.84	1.56	1.27	0.34	1.25
Alternative line shapes								
$f_2(1270)$	0.11	0.10	0.82	0.30	4.05	0.49	4.07	0.45
$f_2(1430)$	0.02	0.04	2.84	1.76	12.05	0.98	6.39	1.05
$\rho(1700)^0$	1.49	0.81	0.75	27.78	4.57	0.73	6.32	0.66
Isobar specifics								
$\sigma$ from PDG	0.01	3.26	2.97	21.83	19.04	0.11	12.9	0.53
Rescattering	0.02	0.14	0.81	0.19	1.97	0.29	1.24	0.17
Total model	1.5	3.5	4.4	35.7	24.1	1.9	16.4	1.9
Statistical uncertainty	1.1	6.5	6.1	3.3	11.4	1.8	8.6	1.7

[Phys. Rev. D 101,012006  
(2020)], [Phys. Rev. Lett. 124  
(2020) 031801]

TABLE VI. Systematic uncertainties on the  $CP$ -averaged fit fractions, given in units of  $10^{-2}$ , for the  $K$ -matrix method. For comparison, the statistical uncertainties are also listed at the bottom.

Category	$\rho(770)^0$	$\omega(782)$	$f_2(1270)$	$\rho(1450)^0$	$\rho_3(1690)^0$	$S$ -wave
$B$ mass fit	1.31	0.01	0.51	0.65	0.04	2.53
Efficiency						
Simulation sample size	0.13	<0.01	0.07	0.09	0.02	0.09
Binning	0.46	<0.01	0.08	0.32	0.07	0.33
L0 trigger	0.02	<0.01	0.01	0.04	<0.01	0.03
Combinatorial bkgd	0.41	0.01	0.15	0.35	0.08	0.24
$B^+ \rightarrow K^+ \pi^+ \pi^-$	0.01	<0.01	<0.01	0.02	<0.01	0.01
Fit bias	0.06	<0.01	0.05	0.09	0.04	0.06
Total experimental	1.5	0.01	0.6	0.8	0.1	2.6
Amplitude model						
Resonance properties	1.02	0.01	0.18	1.41	0.09	0.32
Barrier factors	0.24	<0.01	0.34	0.19	0.06	0.57
Alternative line shapes						
$f_2(1270)$	0.29	0.01	0.62	0.60	0.03	0.05
$f_2(1430)$	2.30	<0.01	2.24	4.17	0.36	0.01
$\rho(1700)^0$	1.66	0.01	0.08	0.55	0.02	0.97
$K$ -matrix specifics						
$s_{\text{prod}}^0$	0.63	<0.01	0.06	0.21	0.03	0.48
$K$ -matrix components	0.48	0.01	0.04	0.36	0.01	0.57
Total model	3.1	0.02	2.4	4.5	0.4	1.4
Statistical uncertainty	0.8	0.04	0.4	0.7	0.1	0.6

[Phys. Rev. D 101,012006  
(2020)], [Phys. Rev. Lett. 124  
(2020) 031801]

TABLE VII. Systematic uncertainties on  $\mathcal{A}_{CP}$  values, given in units of  $10^{-2}$ , for the  $K$ -matrix method. For comparison, the statistical uncertainties are also listed at the bottom.

Category	$\rho(770)^0$	$\omega(782)$	$f_2(1270)$	$\rho(1450)^0$	$\rho_3(1690)^0$	S-wave
$B$ mass fit	1.97	0.12	1.42	9.74	5.77	1.03
Efficiency						
Simulation sample size	0.22	0.88	0.73	0.97	1.34	0.42
Binning	1.53	5.48	0.15	2.89	1.72	1.54
L0 trigger	0.15	0.59	0.19	0.32	0.30	0.02
Combinatorial bkgd	0.61	0.60	1.31	3.45	5.82	0.93
$B^+ \rightarrow K^+ \pi^+ \pi^-$	0.01	0.03	0.03	0.04	0.12	0.03
Fit bias	0.02	0.04	0.24	0.85	0.40	0.36
Total experimental	2.6	5.6	2.1	10.8	8.5	2.1
Amplitude model						
Resonance properties	0.62	0.91	1.08	4.35	5.34	1.27
Barrier factors	1.97	3.54	0.04	12.53	2.79	3.50
Alternative line shapes						
$f_2(1270)$	0.58	0.56	0.48	2.96	4.41	1.13
$f_2(1430)$	3.04	1.69	8.78	41.78	33.96	4.77
$\rho(1700)^0$	3.38	1.17	0.39	8.82	8.80	1.60
$K$ -matrix specifics						
$s_{\text{prod}}^0$	2.08	4.42	0.20	3.42	0.98	2.41
$K$ -matrix components	2.11	5.31	0.01	8.11	0.21	1.03
Total model	5.8	8.1	8.9	45.7	35.9	6.9
Statistical uncertainty	1.5	8.4	4.3	8.4	11.8	2.6

[Phys. Rev. D 101,012006  
(2020)], [Phys. Rev. Lett. 124  
(2020) 031801]

TABLE VIII. Systematic uncertainties on the  $CP$ -averaged fit fractions, given in units of  $10^{-2}$ , for the QMI method. For comparison, the statistical uncertainties are also listed at the bottom.

Category	$\rho(770)^0$	$\omega(782)$	$f_2(1270)$	$\rho(1450)^0$	$\rho_3(1690)^0$	$S$ -wave
$B$ mass fit	1.03	0.03	0.29	0.42	0.01	1.34
Efficiency						
Simulation sample size	0.15	0.01	0.22	0.12	0.02	0.25
Binning	0.03	0.01	0.03	0.21	0.04	0.01
LO trigger	0.04	<0.01	0.01	0.01	<0.01	0.04
Combinatorial bkgd	0.60	0.01	0.19	0.67	0.06	0.62
$B^+ \rightarrow K^+ \pi^+ \pi^-$	0.03	<0.01	0.01	0.02	<0.01	0.03
Fit bias	1.06	0.10	0.46	0.61	0.14	0.68
Total experimental	1.7	0.1	0.7	1.3	0.2	1.8
Amplitude model						
Resonance properties	0.63	0.04	0.21	0.73	0.03	0.18
Barrier factors	0.95	0.05	0.58	0.80	0.04	0.78
Alternative line shapes						
$f_2(1270)$	0.10	0.04	0.30	0.34	0.04	0.36
$f_2(1430)$	0.28	0.01	3.83	0.49	0.04	0.36
$\rho(1700)^0$	0.24	0.01	0.07	0.52	<0.01	0.45
QMI specifics						
QMI bias	0.89	0.11	0.32	3.65	0.47	0.93
Total model	1.4	0.1	3.9	3.8	0.5	1.4
Statistical uncertainty	0.6	0.1	0.4	0.4	0.1	0.6

[Phys. Rev. D 101,012006  
(2020)], [Phys. Rev. Lett. 124  
(2020) 031801]

TABLE IX. Systematic uncertainties on  $\mathcal{A}_{CP}$  values, given in units of  $10^{-2}$ , for the QMI method. For comparison, the statistical uncertainties are also listed at the bottom.

Category	$\rho(770)^0$	$\omega(782)$	$f_2(1270)$	$\rho(1450)^0$	$\rho_3(1690)^0$	$S$ -wave
$B$ mass fit	0.40	1.02	0.23	0.92	0.31	0.04
Efficiency						
Simulation sample size	0.54	1.59	2.29	1.19	0.67	0.46
Binning	0.26	1.46	0.25	1.31	0.87	0.24
L0 trigger	0.15	0.75	0.14	0.07	0.12	0.04
Combinatorial bkgd	0.91	3.05	1.96	10.99	2.88	2.72
$B^+ \rightarrow K^+ \pi^+ \pi^-$	0.01	0.04	0.11	0.33	0.30	0.07
Fit bias	1.92	13.45	5.14	8.24	7.07	2.86
Total experimental	2.3	14.2	6.0	14.3	8.0	4.2
Amplitude model						
Resonance properties	0.47	2.31	0.88	3.23	2.06	1.26
Barrier factors	0.17	3.39	1.99	12.01	3.03	5.12
Alternative line shapes						
$f_2(1270)$	0.02	0.68	0.70	0.98	0.32	0.67
$f_2(1430)$	0.51	0.72	0.08	2.96	1.52	0.67
$\rho(1700)^0$	0.63	2.37	0.97	4.09	0.29	1.39
QMI specifics						
QMI bias	1.35	5.56	4.70	29.40	37.89	4.40
Total model	1.6	7.0	5.2	32.2	38.1	7.0
Statistical uncertainty	1.3	15.4	3.6	5.6	17.0	1.5

[Phys. Rev. D 101,012006  
(2020)], [Phys. Rev. Lett. 124  
(2020) 031801]